FROM THE STRUCTURE AND FUNCTION OF THE RIBOSOME TO NEW ANTIBIOTICS

Nobel Lecture, December 8, 2009

by

THOMAS A. STEITZ

Department of Molecular Biophysics and Biochemistry, Department of Chemistry, Yale University and the Howard Hughes Medical Institute, 266 Whitney Avenue, New Haven, CT 06520-8114, USA.

My passion for pursuing structural studies of biological macromolecules in order to understand how they carry out their functions was initiated by a Dunham lecture that Max Perutz presented at Harvard Medical School in the spring of 1963, a year after he shared the Nobel Prize in Chemistry with John Kendrew for determining the first protein structures. He showed a very large audience the first stereo slide of an atomic structure of a protein, myoglobin, that any of us had ever seen. When the myoglobin structure popped into three dimensions over his head, a loud "oh" came from the audience. I knew then how I wanted to understand the chemistry of biology.

I began my thesis research at Harvard by working with a team in the laboratory of William N. Lipscomb, a Nobel chemistry Laureate in 1976, on the structure of carboxypeptidase A. I did postdoctoral studies with David Blow at the MRC lab of Molecular Biology in Cambridge studying chymotrypsin. My interactions with Jim Watson and with Wally Gilbert while I was at Harvard and the numerous contacts that I had with Francis Crick and Sydney Brenner while I was at Cambridge stimulated my three decade long interest in obtaining the structural basis of Crick's Central Dogma: "DNA makes DNA makes RNA makes Protein". This trail ultimately led to our determining the atomic structure of the large ribosomal subunit, which catalyzes peptide bond formation, as well as the structures of its complexes with substrate analogs and antibiotics.

In the early 1960s, when I was a graduate student, Watson published a figure that summarized what was known about the ribosome structure (Watson, 1963). It showed the A site for the positioning of the aminoacyl-tRNA, though nothing was known about the tRNA structure. The P site located next to the A site had the peptidyl-tRNA, but the pathway taken by the polypeptide product was unknown. Also, the existence of the E site, the exit site, was unknown. In 1976, Jim Lake used electron microscopic studies of negative large and small ribosome subunits as well as the 70S ribosome to obtain the first views of the shapes of the ribosome and its subunits (Lake, 1976). By 1995 Joachim Frank was able to use the single particle cryo-EM methods that he and coworkers had developed to obtain a 25 Å resolution reconstruction of the 70S ribosome with 3 bound tRNA molecules (Frank *et al.*, 1995).

By 1995, my lab had obtained structural insights into the mechanisms of most of the steps of "The Central Dogma", except the last one: protein synthesis by the ribosome. The mid-90s seemed to be the right time to take on this largest of structural biology challenges. Computational power and x-ray crystallographic methodologies including synchrotron x-ray sources and CCD detectors had reached a sufficiently high level to allow x-ray data collection from crystals of such a large assembly. Importantly, Ada Yonath and Wittmann had shown in 1985 that the 50S ribosomal subunit could be crystallized (Shevack *et al.*, 1985), and in 1991 crystals of the *Haloarcula marismortui* (Hma) 50S subunit were obtained that diffracted to 3.0 Å resolution (von Böhlen *et al.*, 1991). The growth of these well-diffracting crystals meant that obtaining the atomic structure of the ribosome was in principle possible. However, while crystals are a necessary condition for determining a crystal structure, they are not sufficient: a large challenge remained – the phasing problem. The 7 Å resolution electron density a map of the Hma 50S subunit that was published in 1995 (Schluenzen *et al.*, 1995) suggested to me (and some others) that the challenge had not yet been correctly met, since the map did not look like RNA. Another approach was needed.

In the fall of 1995 Nenad Ban joined my lab and was interested in pursuing the structure of the ribosome or its component large subunit – the right person at just the right time. I suggested that he tackle the Hma large subunit structure, which he did. I also decided that we should collaborate with a close friend and colleague, as well as one of the pillars of the ribosome research community, Peter Moore. Peter is an avid fisherman who likes to catch big fish, and the ribosome was indeed a big fish. Nenad embarked on determining the structure of the Hma 50S ribosomal subunit with the assistance of Peter's technician, Betty Freeborn, for preparing the subunit. A student in Peter's lab concurrently pursued the objective of crystallization of the 30S subunit or domains of it. By early 1997, Nenad had successfully initiated very low resolution crystallographic studies of the large subunit including the correct location of the heavy atoms in several heavy atom derivatives, when he was then joined in his efforts by Poul Nissen. Through the next three years these two spearheaded the structure determination of the Hma 50S subunit.

While the crystals obtained using the published procedures (von Böhlen *et al.*, 1991) diffracted to 3 Å resolution, they were extremely thin and often multiple. Indeed, Yonath and Franceschi (1998) and Harms *et al.* (1999) described these crystal defects, which included severe nonisomorphism, high radiation sensitivity, nonuniform mosaic spread, uneven reflection shape and high fragility, as well as unfavorable crystal habit. Nissen introduced a back extraction procedure that resulted in isometric and uniform crystals that occasionally diffracted to 2.4 Å resolution (Ban *et al.*, 1999; 2000). Later, Martin Schmeing found an approach that extended the resolution to 2.2 to 2.4 Å more reproducibly (Schmeing *et al.*, 2005a,b). At this resolution the structures, when obtained, can inform on the chemistry of the processes involved in protein synthesis.

What then was the major challenge that needed to be overcome? Why was the determination of the atomic structure of the ribosome perceived to be a very high mountain to climb? The major challenge in determining any crystal structure (once crystals have been obtained) is what is called the "phase problem". Each diffraction spot has an intensity, which can be directly measured, and a phase, which is not directly measurable. Max Perutz was awarded the Nobel Prize in 1962, in part because he developed the method of heavy atom isomorphous replacement to solve the phasing problem for macromolecules. Heavy atoms are bound specifically to the crystal, and their positions in the crystal need to be determined; information that can then be used to obtain the phase angles, which when combined with the diffraction amplitudes allow the calculation of an electron density map.

The phasing challenge presented by the ribosome arises from its large size. Consequently, a single heavy atom provides too weak a diffraction signal to measure and 100 heavy atoms are difficult, if not impossible, to locate. I compare the problem with the challenge of trying to measure the weight of a ship captain by subtracting the weight of the boat from the weight of the boat plus the ship captain. While this can be done with some accuracy for a small sailboat, subtracting the weight of the Queen Mary from that of the Queen Mary plus the captain would give a very small signal, and the ribosome is the Queen Mary of macromolecular assemblies. It is about 100 times heavier than lysozyme.

In order to obtain a super heavy ship captain, Ban used several heavy atom cluster compounds, most importantly one containing 18 tungsten atoms (W_{18}) which together with the other atoms in the compound has about 2,000 electrons. At very low resolution, 20 Å or lower, it scatters almost as one heavy atom. Since the x-ray scatter is proportional to the square of the number of electrons, the scattering signal from the W_{18} cluster compound is over 600 times larger than that from a single 78 electron Tungsten atom. Indeed, its scatter at low resolution is very much larger than that from more than 100 bound Osmium hexamine complexes (Fig. 1).

.

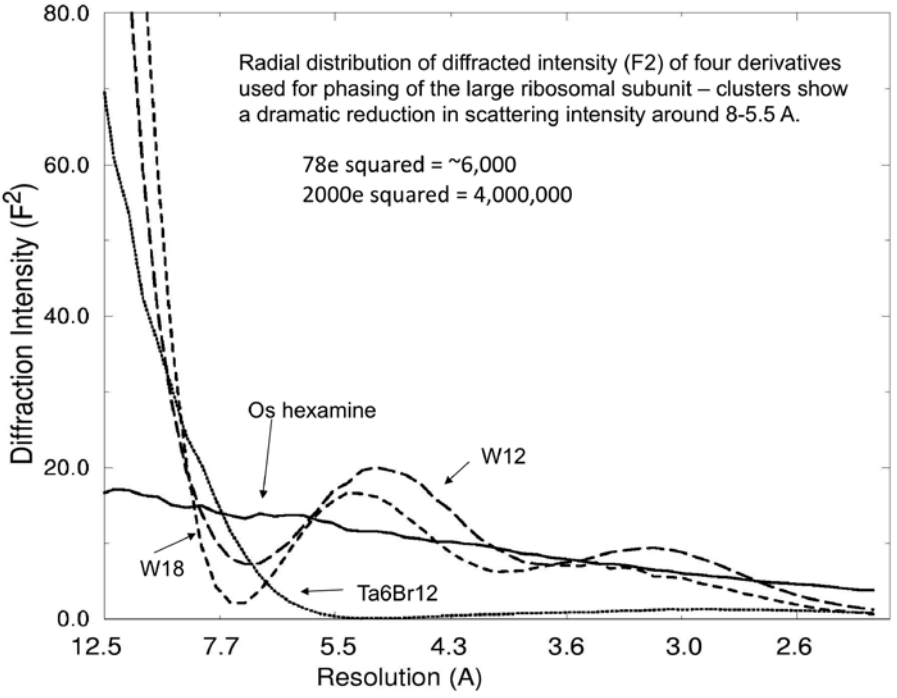

Figure 1. The calculated radial distribution of the scattering intensities produced by four of the heavy atom compounds used for phasing as a function of resolution. At very low resolution the scattering from the cluster compounds, including the W_{18} cluster which contains 2,000 electrons, is extremely large compared with the scatter from more than 100 bound osmium hexamines.

Nenad Ban located the position of a W_{18} cluster compound that was bound to a single site using a 20 Å resolution difference Patterson map (Ban *et al.*, 1998). He then confirmed its location by calculating a difference electron density map, phased using molecular replacement phases derived from a 20 Å resolution cryo-EM map of the Hma 50S subunit provided by Joachim Frank (Fig. 2a). Ban then solved several additional heavy atom cluster compound derivatives using phases derived from the W_{18} derivative. By the end of 2007 he had a very nice 9 Å resolution map of the 50S subunit (Fig. 2b), obtained using only x-ray data, that showed the expected RNA duplex helices and had the same overall shape as seen in the cryo-EM map (Ban *et al.*, 1998).

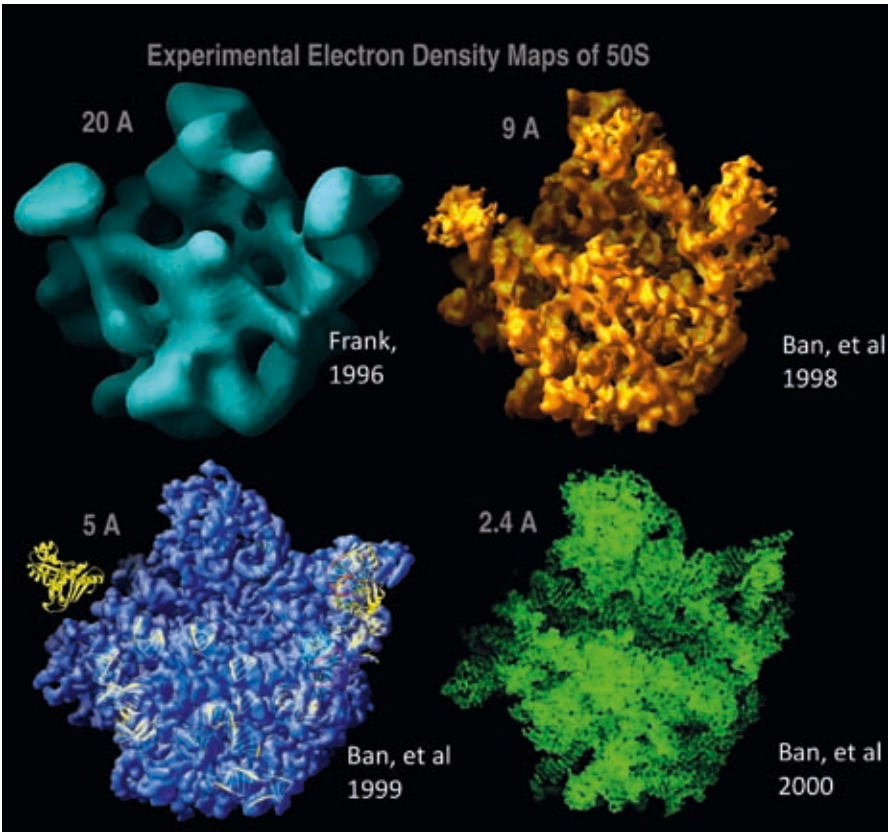

Figure 2. The progressive increase in the resolution of the electron density maps of the 50S ribosomal subunit obtained, beginning with the 20 Å resolution cryo EM map from Joachim Frank (1996) and progressing to our 9 Å resolution map (Ban *et al.*, 1998), which showed the first of the RNA helices, to the 5 Å resolution map (Ban *et al.*, 1999), into which known protein structures could be fitted, and ending with a 2.4 Å resolution map (Ban *et al.*, 2000), which allowed the building of a complete atomic model.

Our strategy during the first four years of our crystallographic studies of the 50S subunit was to work at lower resolutions than 4.5 Å, which could be done using a bending magnet beam line X12C at Brookhaven National Laboratory on Long Island, New York. It was not possible to use the laboratory rotating anode x-ray source because it was too weak, but the X12C source worked fine at low resolutions and was generally very accessible for our use. When finally all of our heavy atom derivatives were made and the heavy atoms correctly located, our first trip to the high intensity insertion device beam line X25 at Brookhaven was made at the end of 1999. Within 4 days, data were collected that allowed calculation of a 3.0 Å resolution map and the initiation of the building of the atomic model.

The resolution of our maps gradually increased from the initial 9 Å resolution (Fig. 2). In 1999, we published a 5 Å resolution map of the 50S Hma subunit in which known r-protein (ribsome protein) structures could be positioned (Ban *et al.*, 1999). In 2000, we published the atomic structure of

the 50S ribosomal subunit derived from a 2.4 Å resolution map calculated using data collected at Argonne National Laboratory (Ban *et al.*, 2000) (Fig. 2d) and that of its complex with a substrate analogue of the transition state of the peptidyl transferase reaction (Nissen *et al.*, 2000). At the same time in 1999 that we published our 5 Å resolution map, the Ramakrishnan group published a 5.5 Å resolution map of the 30S subunit (Clemons *et al.*, 1999) and the Noller group published a 7 Å resolution map of the 70S ribosome (Cate *et al.*, 1999), using phasing approaches that were similar to the cluster approach we published in 1998. Shortly after the appearance of our papers on the 2.4 Å resolution structures of the 50S subunit, two models of the 30S subunit were published (Wimberly *et al.*, 2000; Schleunzen *et al.*, 2000). A year later Noller and colleagues obtained a model of the 70S ribosome with three bound tRNA molecules using a 5.5 Å resolution map into which were fitted the atomic models of the 30S subunit of Ramakrishnan *et al.* and the Hma 50S subunit modified to reflect the eubacterial differences (Yusupov *et al.*, 2001).

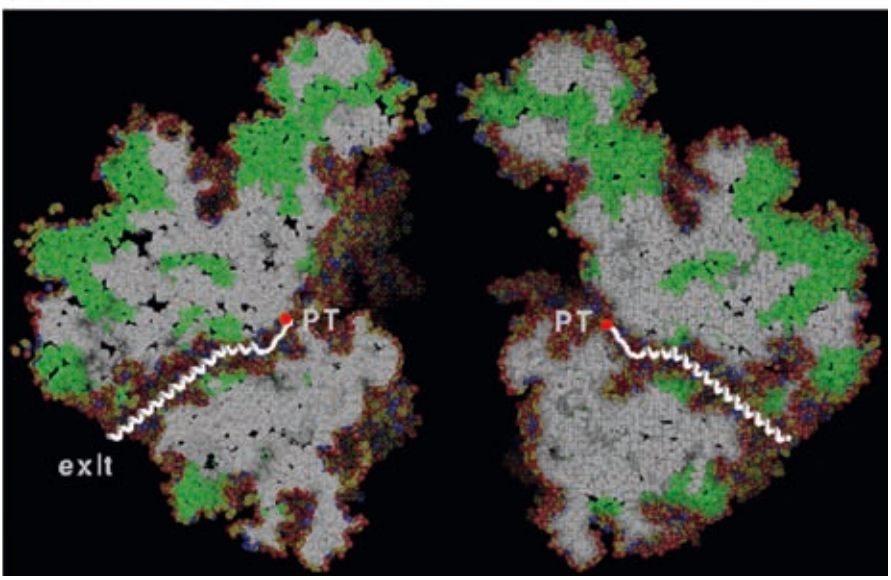

Figure 3. A space filling model of the Hma 50S ribosomal subunit cut in half through its polypeptide exit tunnel at the PTC (PT) and opened up like a book. The tightly packed RNA in the interior is shown in white and the penetrating protein loops in green. A hypothetical model of the exiting polypeptide in the tunnel is shown in white (Nissen *et al.*, 2000).

The 3,000 nucleotides of RNA observed in the Hma 50S subunit exhibited a compact structure with the globular domains of the r-proteins imbedded in its surface, except in the deep cleft where the substrate analogue binds. Splitting the subunit down the middle like an apple and opening it out reveals a 100 Å long polypeptide exit tunnel emanating from the peptidyl transferase center (PTC). It is wide enough to accommodate an alpha-helix

(Nissen *et al.*, 2000; Voss *et al.*, 2006), but not large enough to accommodate any formation of protein tertiary structure as had been proposed (Gilbert *et al.*, 2004). Not only is the packing of the 23S rRNA relatively tight, but extended peptides from many r-proteins are seen to fill the crevices that lie between the RNA helices (Fig. 3). Indeed, when the structures of many of the r-proteins are examined in isolation, they are seen to consist of globular domains and idiosyncratically-folded extended loops and strands that contain many Lys and Arg residues. Two particularly striking examples of extended chains that penetrate deeply into the RNA interior are from r-proteins L2 and L3, which approach the PTC as marked by the bound substrate analogue (Fig. 4).

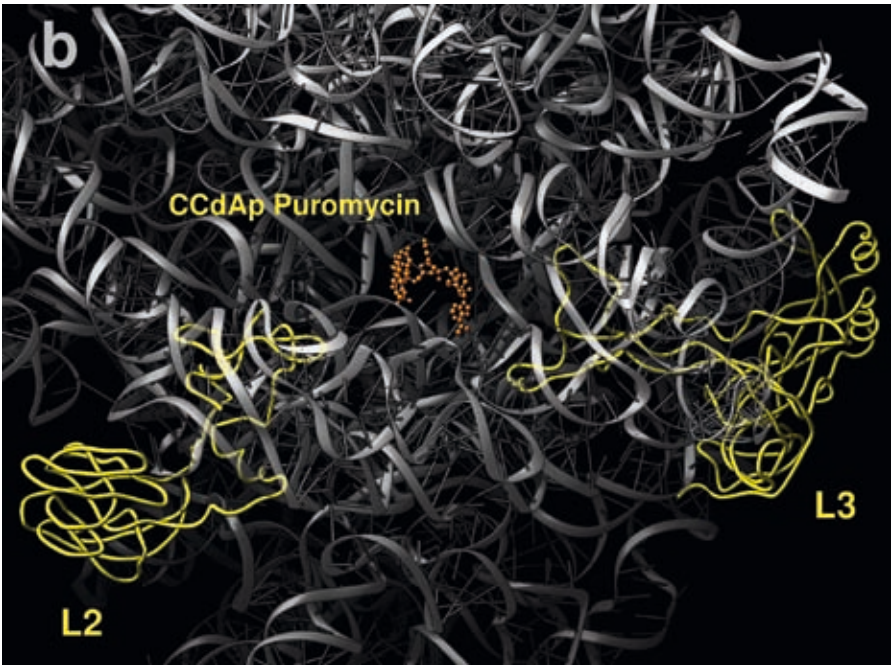

Figure 4. A ribbon representation of the 23S rRNA in white and proteins L2 and L3 in yellow showing the extended peptide chains penetrating into the ribosome interior towards the PTC but not reaching a bound substrate analogue (orange).

Our subsequent analyses of the structural features of the rRNA of the large subunit revealed a novel long-range RNA tertiary structure interaction, the A-minor motif, and a previously unrecognized secondary structure motif, the kink turn (Nissen *et al.*, 2001; Klein *et al.*, 2001). The A-minor motif involves the insertion of the smooth, minor groove (C2-N3) edges of adenine bases within single stranded regions into the minor grooves of neighboring helices, primarily at C-G base pairs. There are 186 adenines in the large subunit observed to make A-minor interactions that stabilize helix-helix, helix-loop, and junction interactions. Ramakrishnan *et al.* subsequently

observed that A-minor interactions are important to decoding by stabilizing correct codon-anticodon interactions (Ogle *et al.*, 2001). The kink-turns (K-turns) are asymmetric internal loops imbedded in RNA double helices. The six K-turns in the Hma 50S subunit have a kink in the phosphodiester backbone that causes a sharp turn in the RNA helix, and they superimpose on each other with an rmsd of 1.7 Å.

Francis Crick had wondered in 1968 whether the catalytic heart of the ribosome was all RNA. Realizing that evolution had faced the "chicken or the egg problem" (which came first?) because the first machine to make a protein could not have been a protein, he wrote "it is tempting to wonder if the first ribosome was made entirely of RNA" (Crick, 1968). Noller and coworkers attempted to establish that indeed the ribosomal RNA is responsible for its catalytic activity by using proteases to digest the r-proteins (Noller *et al.*, 1992). However, many peptides in the 10K molecular weight range, as well as intact L2 and L3, remained. Consequently, this experiment did not confirm the hypothesis that the catalysis is done by the RNA component of the ribosome.

When we examined the positions of all of the proteins that have portions

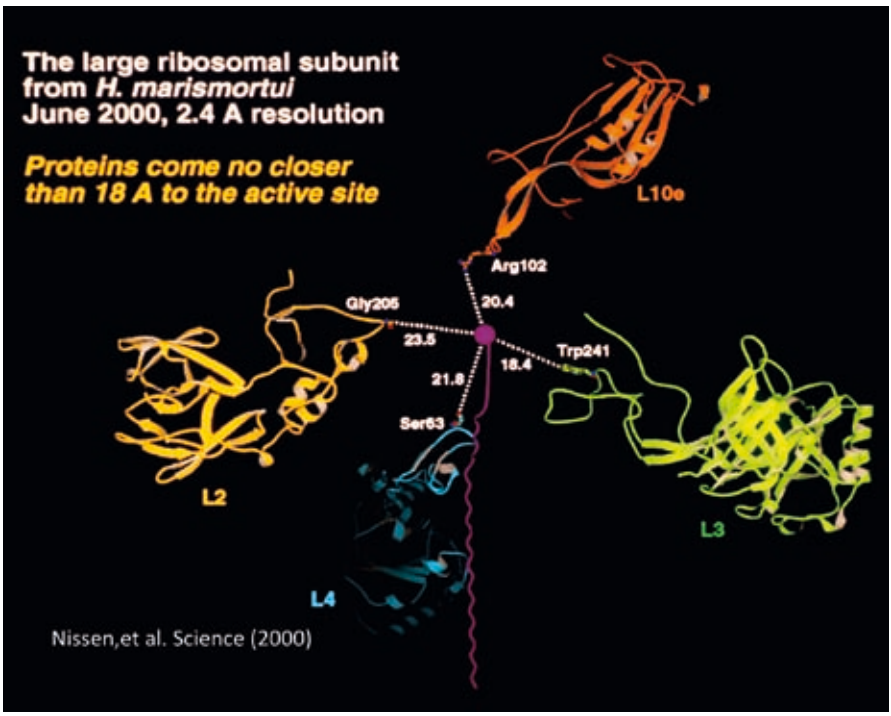

Figure 5. Four proteins whose non-globular extensions into the ribosome interior come the closest to the PTC shown as a red ball, with distances to the PTC given in angstroms (Nissen *et al.*, 2000).

that approach the heart of the PTC, we observed (Fig. 5) in 2000 that the closest protein component lies 18 Å from the PTC (Nissen *et al.*, 2000). Even taking into account that a loop of protein L10e is disordered in this crystal and located in the neighborhood of the PTC, it cannot even hypothetically be extended into the PTC. Therefore, we were led to conclude in 2000 that "The ribosome is a ribozyme". This was the first experimental verification of the hypothesis that had been advocated by many in previous years.

THE MECHANISM OF PEPTIDE BOND FORMATION

As with any enzyme the important question is how catalysis is achieved, and in the case of the ribosome it is of particular interest how RNA can be effective in this process. Of course, as it the case with all enzymes, a major component, if not by far the largest contributor, is the enzyme's capacity to correctly orient the substrates in order that chemistry can occur (Page and Jencks, 1971). This has been shown to be an important component also in ribosome catalysis (e.g., Sievers *et al.*, 2004) . But what other specific chemical mechanisms are utilized?

To address this question, many structures of the Hma large ribosomal subunit complexed with substrate, intermediate and product analogues were determined by Jeff Hansen (Nissen *et al.*, 2000; Hansen *et al.*, 2002) initially and then subsequently by Martin Schmeing (Schmeing *et al.*, 2005a; Schmeing *et al.*, 2005b). The reaction that is catalyzed is the attack of the alpha-amino group of the aminoacyl-tRNA bound in the A site on the carbonyl carbon of the peptidyl-tRNA bound in the P site. This leads to the formation of a tetrahedral carbon that contains an oxyanion; this intermediate then breaks down to form the product peptidyl-tRNA now in the A site and a deacylated P-site tRNA. Since it was not possible to bind full length tRNA substrates to existing crystals of the 50S subunit, we made complexes with fragments of the 3' end of tRNA containing either A, CA or CCA linked to either the amino acid, peptide or analogue of the tetrahedral intermediate. Biochemists had for many years used these kinds of substrate analogues to carry out what is called a "fragment assay" to study the reaction.

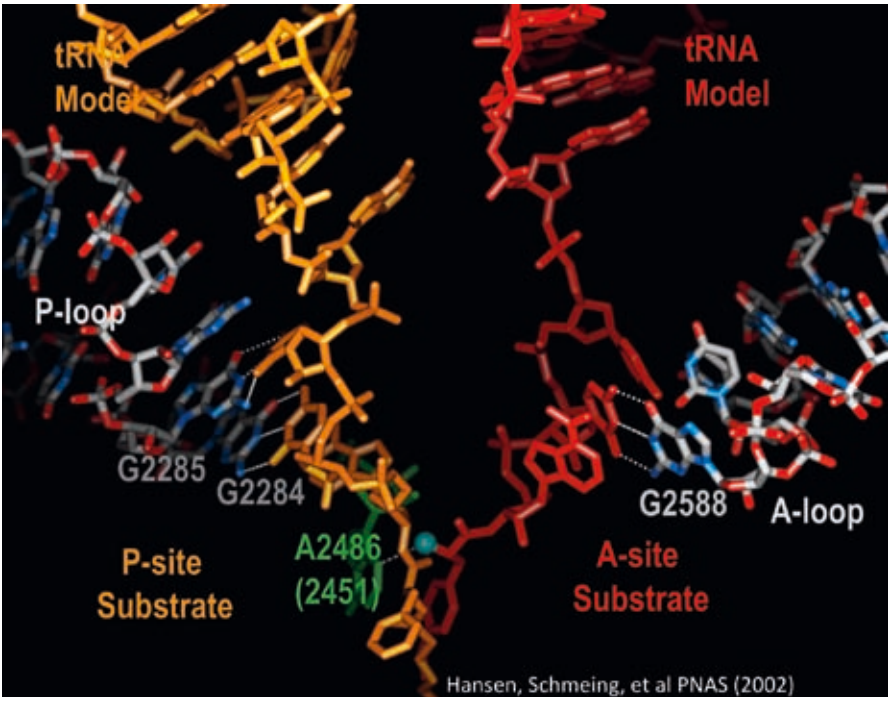

Figure 6. A model of the A-site and P-site substrates bound to the PTC constructed from the structures of the CCA phe cap bio bound to the P site (with sparsomycin, not shown) and C-puromycin bound to the A site, as well as models of the tRNA acceptor stems. The CCA of the P- site substrate makes two base pairs with G2285 and G2284 of the P loop, and C-puromycin makes one base pair with the A loop. The models of the acceptor stems of the A-site and P-site tRNAs are taken from the Yusopov *et al.* (2001) model of the 70S ribosome with tRNAs bound to the A and P sites. The acceptor stems of the two tRNAs are related by a translation, while the 2 CCAs are related by a 180º rotation.

Initially, we determined the structures of substrate complexes with either CC-puromycin bound in the A site or CCA-phe-caproic acid-biotin bound in the P site, which was stabilized in the P site by the simultaneous binding of sparsomycin (Hansen *et al.*, 2002). To construct a model of the structure of a complex with aminoacyl-tRNA bound to the A site and peptidyl-tRNA bound to the P site, the structures of the complexes with the two substrate analogues were built onto the same model of the large subunit. The A- and P-site tRNAs from the Noller *et al.* model of the 70S complex with tRNAs (Yusupov *et al.*, 2001) were also superimposed and joined to the fragment structures (Fig. 6). As had been noted earlier (Nissen *et al.*, 2000), the two tRNA molecules from residue 1 to residue 73 were related by a translation, while their CCA ends were related to each other by a 180º rotation. In the A site, C75 is Watson-Crick base paired to G2588 of the ribosomal A-loop, while in the P site both C74 and C75 make Watson-Crick base pairs to G2285 and G2284 of the P loop. It was suggested (Hansen *et al.*, 2002) that the additional base pair between the CCA and the P loop in the P site as well as base stacking would increase the affinity of the CCA for the P site compared with the A site and

thereby might facilitate the movement of the CCA and of the peptide linked A-site tRNA to the P site once the deacylated P-site tRNA had moved to the E site. These changes in the positions of the CCA ends of the tRNA may be responsible for formation of the hybrid state.

Martin Schmeing then determined the structures of many complexes of the large subunit with substrate analogues of A- and P-site substrates bound simultaneously to the PTC. Together, these suggested the mechanism of peptide bond formation and showed that the premature hydrolysis of the peptidyl-tRNA in the absence of an A-site substrate is suppressed by an induced fit mechanism (Schmeing *et al.*, 2005b). To prepare a stable pre-reaction state complex, the A site substrate used was CC-hydroxypuromycin in which the alpha-amino group is replaced by a less reactive hydroxyl group. In the absence of an A-site substrate, the ester linked carbonyl carbon of peptide linked to the P-site tRNA is protected from a nucleophilic attack by water on both sides by rRNA bases. Addition of the CC-hydroxypuromycin, however, causes a series of conformational changes in the rRNA that lead to the repositioning of the protective base and the reorientation of the carbonyl group positioning it for attack by the alpha-amino group. The structures of these complexes confirm that only the N3 of A2486 (2451 in *E. coli*) and the 2' OH of A 76 of the P-site tRNA contact the attacking alpha-amino group of aminoacyl-tRNA and could be possible candidates for functioning as a general base to activate the nucleophilic attack of the alpha-amino group (Fig. 7). Rachel Green and coworkers showed most conclusively that mutation of A2486 (2451) to any of the three other bases had no effect on the rate of peptide bond formation when full length substrates are used, thereby establishing that A2486 (2451) is not involved in catalyzing peptide bond formation (Youngman *et al.*, 2004).

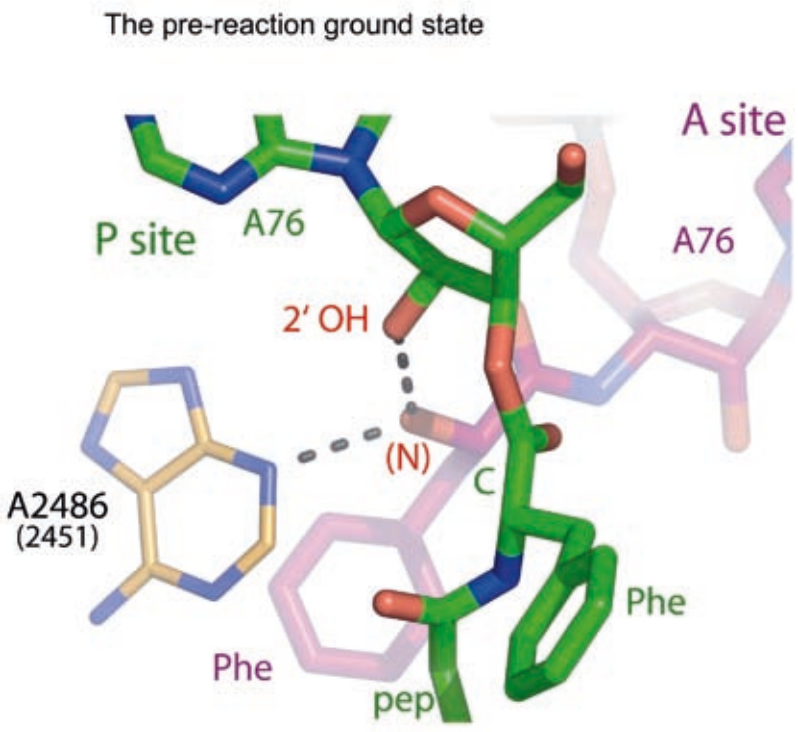

Figure 7. The orientations of two fragment substrates bound to the PTC. The 2'OH of A76 of the P-site substrate in green is the H-bonded to the analogue of the alpha-amino group of the aminoacyl CCA in red. Only the 2'OH of A76 and the N3 of A2486 (2451) interact with the attacking alpha-amino group (Schmeing *et al.*, 2005b).

In contrast, removal of the 2'OH of A76 of the P-site tRNA greatly reduces the rate of the peptidyl transferase reaction. Barta *et al.* found using fragment substrates that remove the 2' OH of A76 of the P-site substrate reduced the rate of peptide bond formation by several hundred-fold (Dorner *et al.*, 2004). Based on this observation and on structures of the Hma 50S subunit complexed with either a P-site substrate analogue or an A-site analogue, Barta proposed that the mechanism of peptide bond formation could be facilitated by a proton shuttle mechanism in which the 2' OH of A76 acts as a general base to receive a proton from the alpha-amino group of the aminoacyl-tRNA to facilitate its nucleophilic attack while simultaneously acting as a general acid to provide a proton to the leaving 3' OH of the P-site A76 upon its deacylation. Strobel and colleagues demonstrated that if full tRNA substrates are used in these studies, then a 2' deoxy-A76 in the peptidyl-tRNA resulted in a rate reduction in peptide bond formation of greater than 10^6 fold (Weinger *et al.*, 2004). Thus, the 2' OH of the P-site tRNA A76 is critical to peptide bond formation.

To explore whether the rate of peptide bond formation is also enhanced by stabilization of the tetrahedral transition state intermediate, Schmeing obtained a 2.3 Å resolution structure of a complex between the Hma 50S subunit and an analogue of the transition state that was synthesized by Kevin Huang in Scott Strobel's laboratory (Schmeing *et al.*, 2005a,b). This analogue had a phosphate mimic of the tetrahedral carbon with an amino acid side chain mimic in place of one of the phosphate oxygens and a sulfur mimic of the oxyanion replacing the second oxygen. Hydrogen bonded to the phosphate oxygen mimic of the oxyanion is a water molecule that is positioned by two rRNA bases (Fig. 8). This water molecule could indeed be assisting in catalysis by partially compensating for the negative charge on the oxyanion.

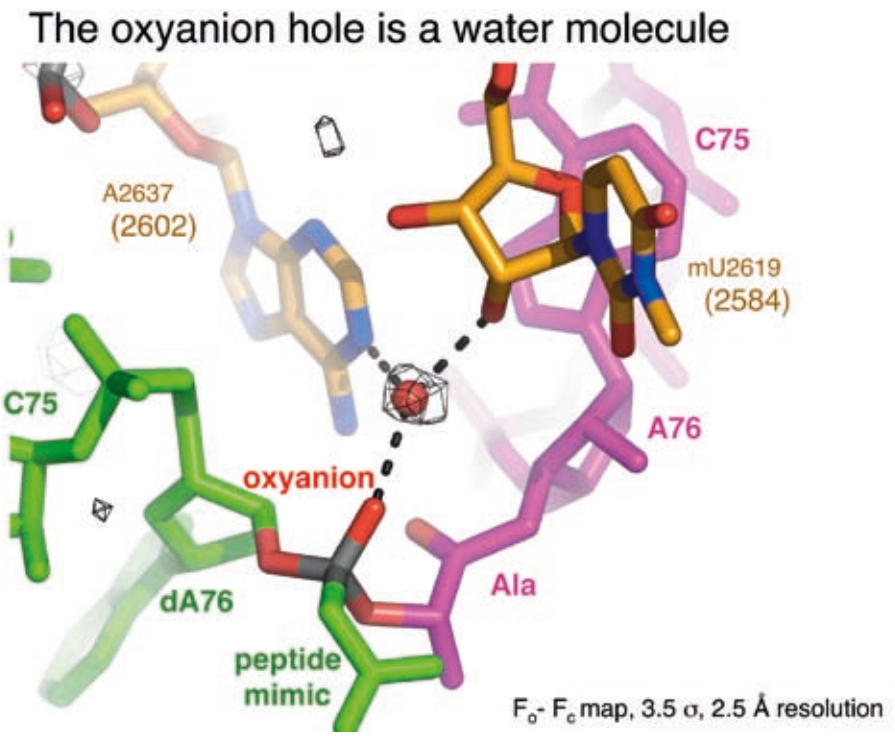

Figure 8. Difference electron density in an F_o-F_c map shows a presumed water molecule H-bonded to the oxyanion mimic of the transition state analogue, as well as to the N6 of A2637 (2502) and to the 2'OH of mU2619 (2585) (Schmeing *et al.*, 2005a).

Consequently, there appear to be at least three contributors to the ribosome's ability to enhance the rate of peptide bond formation. First, it correctly orients the two substrates. Second, it provides substrate assisted catalysis by the 2' OH of A76 of the P-site tRNA that functions as a proton shuttle acting as both a general base and a general acid. Finally, a bound water molecule interacting with the oxyanion may be functioning to stabilize the transition state.

ANTIBIOTIC INHIBITION OF THE 50S RIBOSOMAL SUBUNIT

About 50% of pharmaceutically useful antibiotics target the ribosome and the majority of these bind to the large ribosomal subunit. Our determination of the structure of the Hma large ribosomal subunit has enabled us to obtain the structures of its complexes with many families of antibiotics that bind in or near to the PTC, as well as those that bind in the E site (Hansen *et al.*, 2002; Hansen *et al.*, 2003; Ippolito *et al.*, 2008). Since *H. marismortui* is an archaeon, the antibiotic binding sites of its ribosomes are more similar to those of eukaryotic ribosomes than those of eubacterial ribosomes. Fortunately, at millimolar concentrations many antibiotics that target eubacteria will bind to the Hma large subunit, and our crystal structures of their complexes have enabled the structure-based design of more derivative compounds that are proving effective against resistant bacterial strains. Furthermore, complexes with Hma subunits that have been mutated to contain a eubacterial base bind these antibiotics at pharmacologically relevant concentrations and bind at a position that is displaced by less than an angstrom from that observed for the wild type Hma subunit. Consequently, these observations plus the high resolution of the structural studies that is possible with the Hma crystals have made the Hma large subunit structure a very effective tool in providing structural insights for the design of new antibiotics.

The macrolide family contains many members that have been pharmaceutically important over many years, e.g., erythromycin. The macrolides consist of 14- to 16-membered lactone rings to which various sugar substituents are attached. We were able to establish the structures of complexes with several 16 member macrolides and one 15-member macrolide bound to wild-type 50S subunit (Hansen *et al.*, 2002). The macrolides bind just below the PTC in the polypeptide exit tunnel with the hydrophobic side of the macrolide ring stacking on two splayed-out bases that form a hydrophobic pocket. Although the oligosaccaride substitution on some macrolides, e.g., carbomycin A, overlap the substrate binding sites, most do not. They appear to be functioning by blocking the polypeptide exit tunnel thereby preventing the extension of the elongating polypeptide (Fig. 9). I refer to this process as "molecular constipation". Most of the macrolides interact only with the 23S rRNA and the positions of their macrolide rings superimpose on each other very well. Although there are almost no conformational changes induced in the RNA upon macrolide binding, the 16-member macrolides cause a rotation of the base A 2103 (2100) and form a covalent bond with it.

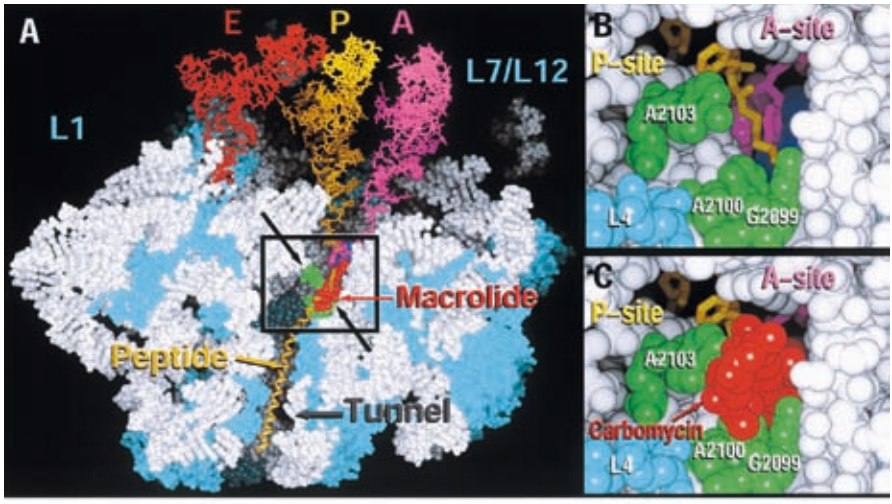

Figure 9. (A) The structure of the macrolide carbomycin (red) bound to the 50S subunit, which is split in half with the 23S rRNA shown in white and the penetrating protein loops in blue (Hansen *et al.*, 2002). The tRNA molecules are derived from combining the tRNA fragment structures complexed with the 50S subunit and the model of the tRNAs bound to the large subunit (Yusupov *et al.*, 2001). (B) A view up the tunnel towards the PTC; the bases whose mutation render the ribosome resistant to inhibition by macrolides are shown in green. (C) The same view as in (B) with the macrolide shown in red in a position that blocks the polypeptide exit.

Aligning the structure of the Hma subunit complexed with azithromycin with that of the *D. radiodurans* subunit bound to erythromycin (Schleunzen *et al.*, 2001) by superimposing their homologous rRNAs shows that the macrolide rings were positioned orthogonally in the two models which seemed surprising for two compounds that are chemically so similar (Hansen *et al.*, 2002). Two possible explanations were posited for this difference initially. One possible cause might be the species differences; the second might be that the erythromycin was mis-positioned in the lower resolution map (3.5 Å) of the Dra complex. Subsequent studies have established that the latter explanation is correct (Tu *et al.*, 2005).

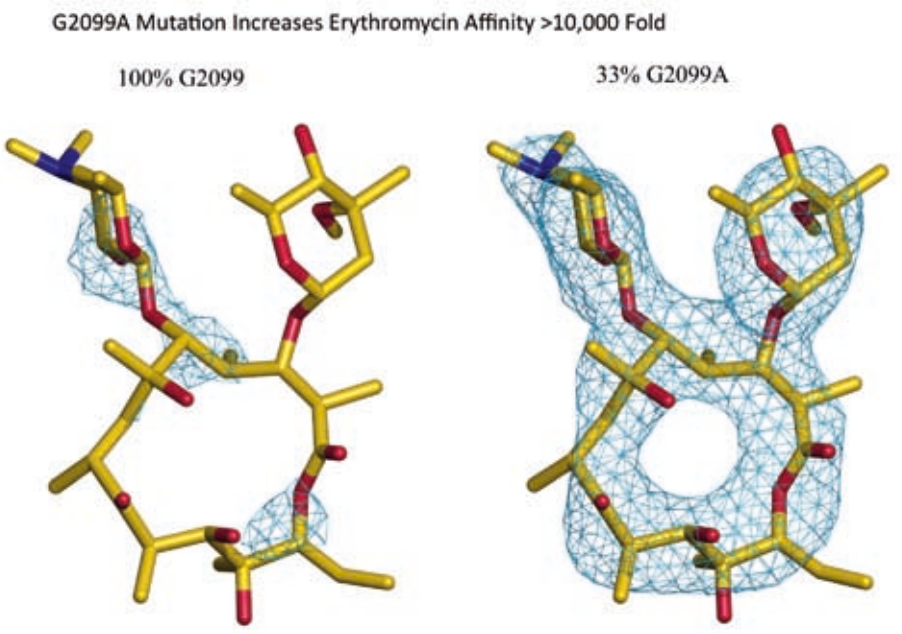

Figure 10. A difference electron density map between the wild-type 50S subunit containing G2099 soaked in 3 mM erythromycin and the apo 50S subunit (left) is compared to a difference map between a G2099A mutant 50S subunit soaked in 0.003 mM erythromycin and the apo-50S subunit (right) (Tu *et al.*, 2005).

Since the major difference between the eubacterial and archaeal binding sites for macrolides is residue A2058 in eubacteria, which is G2099 in archaea and eucaryotes, mutation of A2058 to G in eubacteria reduces the affinity of the ribosomes for erythromycin by about 10^4 fold. Therefore, to better mimic the eubacterial ribosome, G2099 in the Hma 23S rRNA was mutated to an A (Tu *et al.*, 2005). While erythromycin does not bind to the Hma wild-type subunit at 1 mM concentration, it saturates the site of the mutant subunit at 0.001 mM concentration (Fig. 10). Indeed, all antibiotics belonging to the MLS_BK category that do not bind to the wild-type Hma subunit or to a eubacterial 50S subunit having an A2058G mutation bind to the G2099A-mutated Hma 50S subunit. Azithromycin likewise binds at a lower, more physiologically relevant concentration. Its orientation is the same as that observed in the complex with the wild-type 50S subunit, but it is positioned about 1 Å closer to the A2099 (2058) residue due to the lack of steric interference of the N2 of a G residue in that position. Very recently, we have determined the structure at 3.1 Å resolution of erythromycin bound to a 70S *Thermus thermophilus* ribosome and find that it binds identically as erythromycin binds to the mutated Hma 50S subunit (Bulkley, Innis, Blaha, Steitz, unpublished). This further confirms the earlier conclusion that the erythromycin was misoriented in the initial model of the Dra 50S subunit complex (Schluenzen *et al.*, 20001), due presumably to the lower resolution of the electron density map into which the erythromycin was fit.

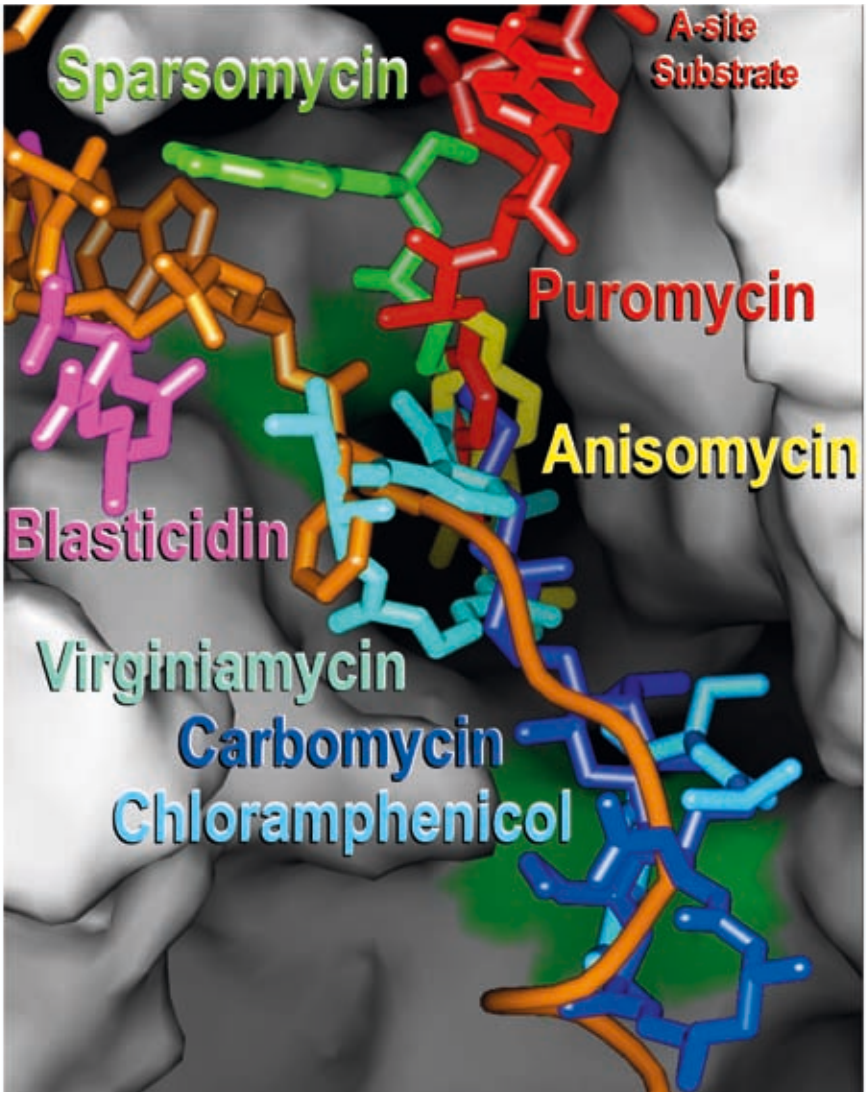

Figure 11. Seven different antibiotics are shown binding to adjacent but distinct binding sites in the PTC. The A site substrate is in red; the P site substrate with an extended peptide model is in orange.

The structures of numerous other complexes between the Hma 50S subunit and different families of antibiotics that bind to the PTC have been determined (Tu *et al.*, 2005; Hansen *et al.*, 2003). Many bind to nearby, but distinct binding sites (Fig. 11) and most inhibit protein synthesis by interfering with the binding of either the P-site or the A-site tRNA. The adjacent locations of these different antibiotic binding sites has provided the opportunity to create novel inhibitors by chemically tying a piece of one antibiotic to a piece of an adjacently-bound one to create hybrid molecules that bind more tightly and provide the starting point for the creation of new antibiotics using computation and structure based design.

DEVELOPMENT OF NEW ANTIBIOTICS BY RIB-X PHARMACEUTICALS, INC.

At a tRNA meeting held in Cambridge, England, in April of 2000, I had a fish and chips lunch with John Abelson at the Eagle Pub, where Francis Crick is reported to have first announced his and Jim Watson's discovery of the structure of double-stranded DNA and its significance for replication. John was a co-founder of Agouron Pharmaceuticals, which in the 1990s used a structure-based drug design approach to create one of the first HIV protease inhibitors; it became an approved pharmaceutical and has been used to successfully treat AIDS as part of combination drug therapy. I asked John if he thought we should start a biotech company to use our structural information on antibiotic complexes with the 50S subunit to design new antibiotic pharmaceuticals effective against resistant bacterial strains, and if so, would he be willing to participate in the founding of such a company? John very excitedly and enthusiastically said yes to both questions. We toasted the future and finished our meal while discussing strategies to explore.

In the following months we began to develop a plan. I asked Peter Moore to join in, which he did, and we decided that we should ask Bill Jorgensen to join the team because of his skills and accomplishments in computational methods of drug design. Susan Froshauer agreed to take on the role of CEO, which she has successfully done to the present time. After raising Angel funding mostly from friends, the company began in the summer of 2001 to use our structures of complexes between the Hma 50S subunit and antibiotics along with Bill Jorgensen's computational methods to carry out structure- and computation-based drug design. The company was named Rib-X Pharmaceuticals, to reflect the rib<u>ribo</u>some target and the use of <u>X</u>-ray crystallography to obtain structures. After eight years, their first drug candidate, radezolid, has successfully completed Phase II clinical trials for use against skin and soft tissue infections and to treat mild-to-moderate community-acquired pneumonia. Other disease applications of radezolid are in Phase II trials and a pipeline of additional compounds is nearing completion of preclinical trials.

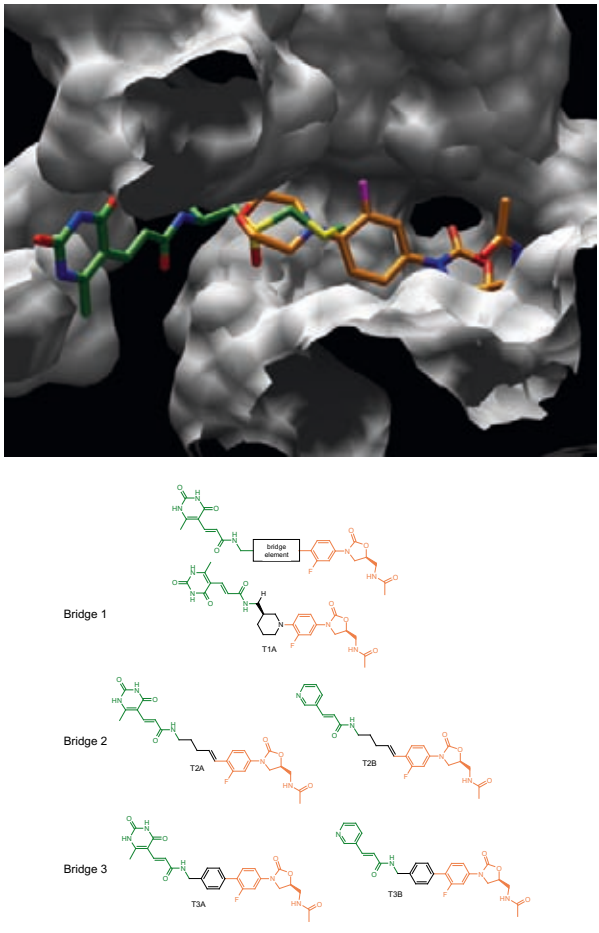

Figure 12. The creation of new hybrid antibiotic compounds by combining (A) sparsomycin on the left (green) with linezolid on the right (orange). The ribosomal RNA to which they bind is shown in a surface representation (grey). (B) These compounds can be chemically linked using various bridge elements to create hybrid compounds.

The design procedures used by Rib-X to ultimately obtain radezolid nicely exemplify how the structures of antibiotic complexes with the 50S subunit and computational methods can be effectively combined with pharmaceutical chemistry and microbiology to create new antibiotics that are effective against antibiotic resistant bacterial strains (Franceschi and Duffy, 2006; Skripkin *et al.*, 2008). Linezolid, an antibiotic sold by Pfizer, binds to the PTC (Ippolito *et al.*, 2008) adjacent to the binding site of the antibiotic sparsomycin (Hansen *et al.*, 2003), which is not selective between eubacteria and eucaryotes (Fig. 12a). In this example, portions of the two antibiotics are chemically linked together to create five new compounds whose intrinsic affinity, kingdom selectivity and minimum inhibitory concentrations (MIC) are measured (Fig. 12b; Table 1). Two of the five were selective for eubacteria, showing that replacement of the key sparsomycin affinity element could alter

the selectivity without completely losing ribosomal binding. Furthermore, the pair on the right (T3A and T3B) featuring the biaryl template showed not only substantially improved intrinsic affinity, but also dramatic improvement in antibacterial activity against representative community and nosocomial drug-resistant strains. With this proof-of-concept established, completely new molecules were designed. These took advantage of the ribosomal space defined by the chimeras, and they were optimized within these boundaries using computational methods to balance the molecular features so that Gram-positive and Gram-negative membranes could be penetrated, solubility and permeability could be maximized for oral bioavailability, and liabilities that might relate to toxicity were avoided. After synthesis of fewer than 700 compounds within less than one year's time, two drug candidates emerged: these featured greater than 10^3 lower inhibitory concentration for eubacteria than eucaryotes, very low MICs (0.25 and 2) against drug-resistant *S. pneumoniae* and *H. influenzae,* and oral efficacy in a variety of rodent models of infection. The final selected compound, radezolid, was found to be significantly more effective against many antibiotic resistant strains than the parent linezolid compound.

	Linezolid (Lin)	Sparsomycin (Spa)	RX-154	RX-190	RX-209	RX-212	RX-213
Intrinsic Affinity (Cell-Free Translation Inhibition)							
E. coli D10 IC_{50} (μM)	4.6	<0.02	0.26	0.03	16	0.03	0.58
Bacterial Selectivity	Y	N	N	N	Y	N	Y
Antibacterial Activity (MICs in μg/mL)							
S. pneumoniae O2J1175 (Mac^R, efflux)	2	2	4	1	8	<0.25	0.5
S. pyogenes Msr610 (Mac^R, rRNA methylation)	1	2	4	1	4	<0.25	0.5
E. faecalis P5 (Lin^R, G2576U)	>32	>128	>128	32	>128	16	16

Table 1. The minimum inhibitory concentrations (MICs) against three bacterial strains exhibited by five compounds created by chemically combining sparsomycin with linezolid.

An analogous approach has led to the creation of a family of enhanced macrolides. This family features representatives of the 14-, 15- and 16-membered macrolide families that have been augmented in novel ways to access adjacent, validated binding sites in the Hma 50S ribosome. By so doing, they not

only restore activity against bacterial strains that are macrolide-resistant (e.g., the streptococci and the staphylococci, including community- and hospital-acquired MRSA), but also extend the spectrum to be effective against other drug-resistant Gram-positive bacteria such as the vancomycin-resistant enterococci. These compounds are in the late-stages of preclinical testing.

Building on the knowledge that was derived from those programs, the Rib-X team undertook the *de novo* design of completely new antibiotics that target the 50S ribosomal subunit. Not only do they represent new classes for this important target, but also they have been optimized computationally to show potency against strains of multidrug-resistant Gram-negative organisms like *Escherichia coli*, *Psuedomonas aeruginosa* and *Acinetobacter baumannii*. Additionally, because these compounds represent new chemical classes, they should not be affected by known resistance mechanisms seen clinically for other antibiotics. Thus, it appears that the structure of the Hma large ribosomal subunit and those of its complexes with antibiotics are enabling the development of a pipeline of new potential antibiotics.

NEW ANTIBIOTICS AGAINST TUBERCULOSIS?

Tuberculosis (TB) continues to be a major disease that causes over a million deaths a year, primarily in the poorest regions of the world. Also troubling is the recent emergence of strains, called XDR, that are resistant to all anti-TB antibiotics regardless of their specific molecular target. The possible spread of the XDR strains poses a potential medical problem for the rest of the world as well.

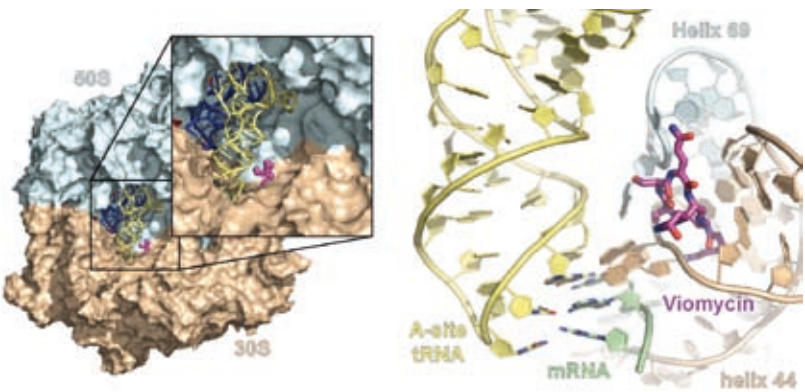

Figure 13. The binding site for viomycin at the decoding center interacting with RNA from both subunits (Stanley *et al.*, 2010). Shown on the left is a surface rendition of the 70S ribosome with the 50S subunit in blue, the 30S subunit in tan, the A-site tRNA in yellow and viomycin in red. A close-up view of viomycin bound to the large subunit helix 69 and small subunit helix 44 at the decoding center; stabilizing bases 1492 and 1493 are in their "flipped out" conformation, making A minor interactions with the codon of the mRNA (green) base-paired with the anticodon of the tRNA (yellow).

We have recently (Stanley *et al.*, 2010) determined the structures of the 70S *Thermus thermophilus* ribosome complexed with tRNA molecules bound to the A, P and E sites as well as capreomycin and viomycin, two tuberactinomycin cyclic peptide antibiotics effective against TB. They were known to bind only to the 70S ribosome and we observe them between the two subunits near the decoding center, interacting with tRNA and the beta 2A intersubunit bridge, which is formed by the contact between large subunit helix 69 and small subunit helix 44. The drugs interact with bases A1492 and A1493, stabilizing them in the "flipped out" orientation that they assume when assisting in mRNA decoding. It appears that the drugs stabilize the tRNA in the pre-translocation state (Fig. 13).

Importantly, the capreomycin/viomycin binding site lies adjacent to the binding sites for two antibiotics that bind the small subunit, paromomycin (Voorhees *et al.*, 2009) and hygromycin B (Borovinsaya *et al.*, 2008) (Fig. 14). This provides the opportunity to apply the same approach that Rib-X has been successfully employing to develop new anti-TB antibiotics by chemically tying a portion of either hygromycin B or paromomycin to capreomycin. Since the XDR strain may be the consequence of a mutation in an ionpump a new, larger compound might prove effective.

Viomycin, hygromycin & paromomycin bind to adjacent sites

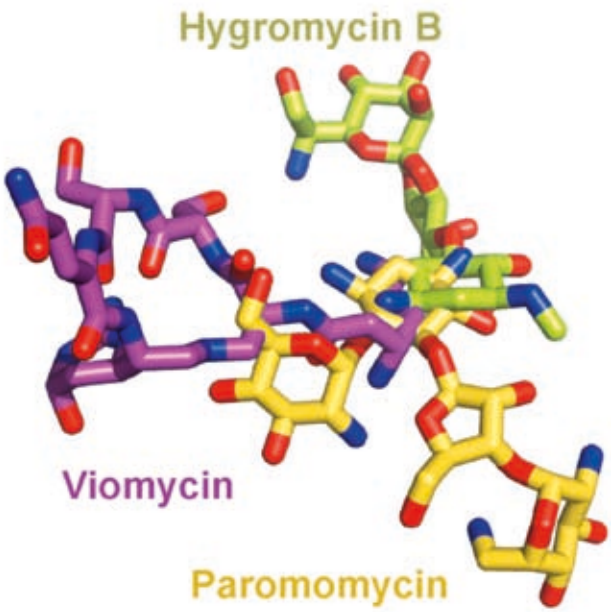

Figure 14. The adjacent binding sites of viomycin (purple), hygromycin B (green) and paromomycin (yellow) at the decoding center open the possibility of combinational drug design of new anti-TB antibiotics (Stanley *et al.*, 2010).

CONCLUSION

We began our structural studies of the ribosomal large subunit in order to learn how this largest of RNA machines is built and how it is able to catalyze peptide bond formation. These basic science questions and answers have led to a practical and applied outcome that uses the power of structural and computational methods to design new potential antibiotics that are effective against antibiotic resistant bacterial strains. Our work reinforces my view of the importance of research funding agencies continuing to emphasize their support of basic research rather than divert their efforts to "translational" research, which I believe has a more limited horizon for novel discoveries.

ACKNOWLEDGMENTS

I acknowledge the important contributions to the structural studies of the ribosome of all of the members of my research group as well as Peter Moore's group, during the past 15 years in addition to the four who are specifically mentioned in the text. I also wish to acknowledge the unique and enabling research environment created by the seven Center for Structural Biology (CSB) laboratories at Yale between 1995 to 2000 (Richards, Engelman, Moore, my lab, Sigler, Brünger and Doudna). Importantly, the long term and major support of my lab research and of the CSB by the Howard Hughes Medical Institute has been vital to the success of our studies of the ribosome. Support was also provided by a program project grant from the NIH. Finally, Erin Duffy assisted in the writing of the summary of drug development by Rib-X Pharmaceuticals, Inc.

REFERENCES

1. Ban, N., Freeborn, B., Nissen, P., Penczek, P., Grassucci, R. A., Sweet, R., Frank, J., Moore, P. B. and Steitz, T. A. (1998), "A 9 Å resolution X-ray crystallographic map of the large ribosomal subunit," *Cell* **93**, 1105–1115.
2. Ban, N., Nissen, P., Hansen, J., Capel, M., Moore, P.B. and Steitz, T.A. (1999), "Placement of protein and RNA structures into a 5 Å resolution map of the 50S ribosomal subunit," *Nature* **400**, 841–847.
3. Ban, N., Nissen, P., Hansen, J., Moore, P. B. and Steitz, T. A. (2000), "The complete atomic structure of the large ribosomal subunit at 2.4 Å resolution," *Science* **289**, 905–920.
4. Borovinsaya, M.S., Shoji, S., Fredrick, K., and Cate, J.H. (2008), "Structural basis of a hygromycin B inhibition of protein biosynthesis," *RNA* **14**, 1590–1599.
5. Carter, A. P., Clemons, W. M., Brodersen, D. E., Morgan-Warren, R. J., Wimberly, B. T. and Ramakrishnan, V. (2000), "Functional insights from the structure of the 30S ribosomal subunit and its interactions with antibiotics," *Nature* **407**, 340–348.
6. Cate, J. H., Yusupov, M. M., Yusupova, G. Z., Earnest, T. N. and Noller, H. F. (1999), "X-ray crystal structures of 70S ribosome functional complexes," *Science* **285**, 2095–2104.
7. Clemons, W.M., May, J.L.C., Wimberly, B.T., McCutcheon, J.P., Capel, M.S., Ramakrishnan, V. (1999), "Structure of a bacterial 30S ribosomal subunit at 5.5 Å resolution," *Nature* **400**: 833–840.
8. Crick, F. H. C. (1968), "The origin of the genetic code," *J. Mol. Biol.* **38**, 367–379.
9. Dorner, S., Panuschka, F., Schmid, W. and Barta, A. (2003), "Mononucleotide derivatives as ribosomal P-site substrates reveal an important contribution of the 2'-OH activity," *Nucl. Acids Res.* **31**, 6536–6542.
10. Franceschi, F., Duffy, E.M. (2006), "Structure-based drug design meets the ribosome," *Biochemical Pharmacology* **71**, 1016–1025.
11. Frank, J., Zhu, J., Penczek, P., Li, Y., Srivastava, S., Verschoer, A., Radermacher, M., Grassucci, R., Lata, R.K., Agrawal, R.K. (1995), "A model of protein synthesis based on cryo-electron microscopy of the *E. coli* ribosome," *Nature* **376**, 441–444.
12. Hansen, J.L., Schmeing, T.M., Moore, P.B. and Steitz, T.A. (2002), "Structural insights into peptide bond formation," *Proc. Natl. Acad. Sci. USA* **99**, 11670–11675.
13. Hansen, J.L., Moore, P.B. and Steitz, T.A. (2003), "Structure of five antibiotics bound at the peptidyl transferase center of the large ribosomal subunit," *J. Mol. Biol.* **330**, 1061–1075.
14. Harms, J., Tocilj, A., Levin, I., Agmon, I., Stark, H., Kölln, I., van Heel, M., Cuff, M., Schlünzen, F., Bashan, A., Franceschi, F. and Yonath, A. (1999), "Elucidating the medium-resolution structure of ribosomal particles: an interplay between electron cryo-microscopy and X-ray crystallography," *Structure* **7**, 931–941.
15. Ippolito, J.A., Kanyo, Z.F., Wang, D., Franeschi, F.J., Moore, P.B., Steitz, T.A., and Duffy, E.M. (2008), "Crystal structure of the oxazolidinone antibiotic linezolid bound to the 50S ribosomal subunit," *J. Med. Chem.* **51**, 3353–3356.
16. Klein, D.J., Schmeing, T.M., Moore, P.B. and Steitz, T.A. (2001), "The kink-turn: a new RNA secondary structure motif," *The EMBO J.* 4214–4221.
17. Lake, J.A. (1976), "Ribosome structure determined by electron microscopy of *Escherichia coli* small subunits, large subunits and monomeric ribosomes," *J. Mol. Biol.* **105**, 131–159.
18. Nissen, P., Ban, N., Hansen, J., Moore, P. B. and Steitz, T. A. (2000), "The structural basis of ribosome activity in peptide bond synthesis," *Science* **289**, 920–930.
19. Nissen, P., Ippolito, J. A., Ban, N., Moore, P. B. and Steitz, T. A. (2001), "RNA tertiary interactions in the large ribosomal subunit: the A-minor motif," *Proc. Natl. Acad. Sci. USA* **98**, 4899–4903.
20. Noller, H.F., Hoffarth, V. and Zimniak, L. (1992), "Unusual resistance of peptidyl transferase to protein extraction procedures," *Science* **256**, 1416–1419.

21. Ogle, J. M., Brodersen, D. E., Clemons, W. M., Tarry, M. J., Carter, A. P. and Ramakrishnan, V. (2001), "Recognition of cognate transfer RNA by the 30S ribosomal subunit," *Science* **292**, 897–902.
22. Page, M.I. and Jencks, W.P. (1971), "Entropic contributions to rate acceleration in enzymatic and intramolecular reactions and the chelate effect," *Proc. Natl. Acad. Sci. USA* **68**, 1678–1683.
23. Schlünzen, F., Hansen, H.A.S., Thygesen, J., Bennett, W.S., Volkmann, N., Levin, I., Harms, J., Bartels, H., Zaytzev-Bashan, A., Berkovitch-Yellin, Z., Sai, I., Franceschi, F., Krumbholz, S., Geva, M., Weinstein, S., Agmon, I., Böddeker, N., Morlang, S., Sharon, R., Dribin, A., Maltz, E., Peretz, M., Weinrich, V. and Yonath, A. (1995), "A milestone in ribosomal crystallography: the construction of preliminary electron density maps at intermediate resolution," *Biochem. Cell Biol.* **73**, 739–749.
24. Schluenzen, F., Tocilj, A., Zarivach, R., Harms, J., Gluehmann, M., Janell, D., Bashan, A., Bartles, H., Agmon, I., Franceschi, F. *et al.* (2000), "Structure of functionally activated small ribosomal subunit at 3.3 Å resolution," *Cell* **102**, 615–623.
25. Schleunzen, F., Zarivach, R., Harms, J., Bashan, A., Tocilj, A., Albrecht, R., Yonath, A. and Franceschi, F. (2001), "Structural basis for the interaction of antibiotics with the peptidyl transferase centre in eubacteria," *Nature* **413**, 814–821.
26. Schmeing, T.M., Kitchen, D., Scaringe, S.A., Strobel, S.A. and Steitz, T.A. (2005a), "Structural insights into the roles of water and the 2' hydroxyl of the P-site tRNA in the peptidyl transferase reaction," *Molec. Cell* **20**, 437–448.
27. Schmeing, T.M., Huang, K.S., Strobel, S.A., and Steitz, T.A. (2005b), "An induced-fit mechanism to promote peptide bond formation and exclude hydrolysis of peptidyl tRNA," *Nature* **438**, 520–524.
28. Shevack, A., Gewitz, H.S., Hennemann, B., Yonath, A. and Wittmann, H.G. (1985), "Characterization and crystallization of ribosomal particles from *Halobacterium marismortui*," *FEBS* **184**, 68–71.
29. Sievers, A., Beringer, M., Rodnina, M.V., Wolfenden, R. (2004), "The ribosome as an entropy trap," *Proc. Natl. Acad. Sci. USA* **101**, 7897–7901.
30. Skripkin, E., McConnell, T.S., Devito, J., Lawrence, L., Ippolito, J.A., Duffy, E.M., Sutcliffe, J., Franceschi, F. (2008), "Rχ-01, a new family of oxazolidinones that overfcome ribosome-based linezolid resistance," *Antimicrobial Agents and Chemotherapy* **52**, 3550–3557.
31. Stanley, R.E., Blaha, G., Grodzicki, R.L., Strickler, M.D. and Steitz, T.A. (2010), "The structures of the anti-tuberculosis antibiotics viomycin and capreomycin bound to the 70S ribosome," *Nature Struct. and Molec Biol.* 17, 289–293.
32. Tu, D., Blaha, G, Moore, P.B. and Steitz, T.A. (2005), "Structures of MLSbK antibiotics boundto mutated large ribosomal subunits provide a structural explanation for resistance," *Cell* **121**, 257–270.
33. von Böhlen, K., Makowski, L., Hansen, H.A.S., Bartels, H., Berkovitch-Yellin, Z., Zaytzev-Bashan, A., Meyer, S., Paulke, C., Franceschi, F., and Yonath, A. (1991), "Characterization of preliminary attempts for derivatization of crystals of large ribosomal subunits from *Haloarcula marismortui*, diffraction to 3 Å resolution," *J. Mol. Biol.* **222**, 11–15.
34. Voorhees, R.M., Weixlbaumer, A., Loakes, D., Kelley, A.C. and Ramakrishnan, V. (2009), "Insights into substrate stabilization from snapshots of the peptidyl transferase center of the intact 70S ribosome," *Nature Struc. Biol.* **16**, 528–533.
35. Voss, N.R., Gerstein, M., Steitz, T.A., and Moore, P.B. (2006), "The geometry of the ribosomal polypeptide exit tunnel," *J. Mol. Biol.* **360**, 893–906.
36. Watson, J. D. (1963), "Involvement of RNA in the synthesis of proteins," *Science* **140**, 17–26.
37. Weinger, J.S., Parnell, K.M., Dorner, S., Green, R. and Strobel, S.A. (2004), "Substrate-assisted catalysis of peptide bond formation by the ribosome," *Nature Struc. Biol.* **11**, 1101–1106.

38. Wimberly, B. T., Brodersen, D. E., Clemons, W. M., Morgan-Warren, R. J., Carter, A. P., Vonrhein, C., Hartsch, T. and Ramakrishnan, V. (2000), "Structure of the 30S ribosomal subunit," *Nature* **407**, 327–339.
39. Youngman, E.M., Brunelle, J.L., Kochaniak, A.B., and Green, R. (2004), "The active site of the ribosome is composed of two layers of conserved nucleotides with distinct roles in peptide bond formation and peptide release," *Cell* **117**, 589–599.
40. Yonath, A., Franceschi, F. (1998), "Functional universality and evolutionary diversity: insights from the structure of the ribosome," *Structure* **6,** 679–684**.**
41. Yusupov, M. M., Yusupova, G. Z., Baucom, A., Lieberman, K., Earnest, T. N., Cate, J. H. D. and Noller, H. F. (2001), "Crystal structure of the ribosome at 5.5 Å resolution," *Science* **292**, 883–896.

Portrait photo of Professor Steitz by photographer Ulla Montan.